Pergamon

PII: S1359-6454(97)00136-5

CREEP OF METALS CONTAINING HIGH VOLUME FRACTIONS OF UNSHEARABLE DISPERSOIDS—PART II. EXPERIMENTS IN THE Al–Al$_2$O$_3$ SYSTEM AND COMPARISON TO MODELS

A. M. JANSEN† and D. C. DUNAND‡

Department of Materials Science and Engineering, Massachusetts Institute of Technology, Cambridge, MA 02139, U.S.A.

Abstract—The tensile and compressive creep properties of coarse- and fine-grained dispersion-strengthened aluminum with 25 vol.% submicron alumina dispersoids are presented for temperatures between 335°C and 500°C and stresses between 30 MPa and 110 MPa. For all stresses investigated, the minimum creep rate is higher in tension than in compression, because cavitation is the main deformation mechanism in tension. In compression, however, dislocation creep is the dominant deformation mechanism at all stresses for the large-grained material and at high stresses for the fine-grained material, while diffusional creep dominates in the fine-grained material at low stresses. The apparent stress exponents for both diffusional creep and dislocation creep are much higher than for unreinforced aluminum, indicating that the dispersoids strongly inhibit both mechanisms. The threshold stresses determined experimentally for dislocation creep are significantly higher than those predicted by existing climb or detachment models, which consider the interaction of a single dislocation with dispersoids. Since transmission electron microscopy reveals that several dislocations typically interact with a single dispersoid, the modified threshold stress model presented in the theoretical companion article [1] is applicable, whereby the stress of dislocation pile-ups upon the threshold-controlling dislocation is taken into account. Good agreement is found between the experimentally determined threshold stresses and theoretical predictions from that model. The same model can also satisfactorily explain the very high measured values of the apparent activation energy. © *1997 Acta Metallurgica Inc.*

1. INTRODUCTION

Large improvements in creep strength can be achieved in metals by the addition of non-shearable, submicron dispersoids exhibiting chemical compatibility with the matrix and low coarsening tendency. Dispersion-strengthening in metals results from dispersoids impeding the motion of matrix dislocations within the grains or at grain boundaries [2–5]. The steady-state minimum creep rate $\dot{\epsilon}$ of most dispersion-strengthened metals can be described by a power-law equation:

$$\dot{\epsilon} = A'\sigma^{n'} \exp\left(\frac{-Q'}{RT}\right) \tag{1}$$

where σ is the applied tensile stress, n' the apparent stress exponent, Q' the apparent activation energy, R the gas constant, T the absolute temperature and A' is a function of the shear modulus and temperature. At stresses below the power-law breakdown region,

†Present address: Arthur D. Little, Inc. Cambridge, MA 40, U.S.A.; previously known as A. M. Redsten.
‡Present address: Department of Materials Science and Engineering, Northwestern University, Evanston, IL 60208, U.S.A.

the creep rate of dispersion-strengthened metals is much lower than that of the unreinforced matrix, but the stress-sensitivity n' and temperature-sensitivity Q' are much higher. This behavior is usually justified by invoking an athermal threshold stress σ_{th} below which dislocation motion does not occur. Modifying equation (1) to account for the threshold stress gives:

$$\dot{\epsilon} = A[\sigma - \sigma_{th}]^n \exp\left(\frac{-Q}{RT}\right) \tag{2}$$

where A is a constant containing the shear modulus and the temperature and n and Q are the stress exponent and activation energy of the unstrengthened matrix, respectively.

When a matrix dislocation blocked by a particle overcomes the obstacle by climbing over it, a threshold stress arises because the dislocation increases its length during the climb process. In the local climb model [6–8], the non-climbing portion of the dislocation remains in the slip plane while the climbing portion assumes the shape of the particle. A computer simulation of local climb over spherical particles [8] led to a threshold stress σ_{loc} given by

$$\sigma_{loc} = 0.4 \cdot \sigma_{or} \tag{3}$$

where σ_{or} is the Orowan stress given in equation (3) of the theoretical companion article [1]. In the general climb model [9], part of the dislocation line between neighboring particles climbs out of the slip plane. The diffusional mass transport required to sustain that mechanism is increased, but the threshold stress is reduced compared to the local climb model, because the total dislocation line length is decreased by a factor κ, given by McLean [10] as a function of the volume fraction f. The general climb threshold stress σ_{gen} is then:

$$\sigma_{gen} = 0.4 \cdot \kappa \cdot \sigma_{or}. \qquad (4)$$

At high particle volume fractions, it is energetically more favorable for a single dislocation to overcome groups of particles rather than threading between individual particles. McLean [10] presented a model for the backstress σ_{coop} owing to this so-called cooperative climb mechanism, which for a tensile stress applied at $\theta = 45°$ to the surface normal is given by

$$\sigma_{coop} = \sigma[1 + \sqrt{1 + (f^{-1/3} - 1)^2}]^{-1} \qquad (5)$$

and is independent of the particle size and interparticle spacing, but proportional to the applied stress σ.

After the dislocation has climbed over the particle, it may still need to overcome another barrier associated with the attractive nature of an incoherent interface between particle and matrix [11]. The resulting detachment threshold stress σ_{det} is given by Arzt and Wilkinson [12] as

$$\sigma_{det} = \zeta \sqrt{1 - k^2} \sigma_{or} \qquad (6)$$

where k is the relaxation factor (defined as the ratio between the dislocation line energies at the particle–matrix interface and within the bulk matrix). As described in the theoretical companion article [1], the factor $\zeta = \bar{\lambda}/L$ (where $\bar{\lambda}$ is the mean interparticle distance and L is the center-to-center particle distance) is used to harmonize the notation with the other threshold equations. While deformation is possible at stresses below the detachment threshold stress by thermal activation [13], the resulting creep strain rate is not experimentally measurable if the relaxation factor is less than about $k = 0.9$; equation (6) can then be considered as an athermal threshold stress.

The creep properties of metals containing low volume fractions (typically less than 10 vol.%) of submicron unshearable dispersoids has been extensively studied for aluminum-based materials, e.g. with sintered aluminum powders (SAP) [14–16] and mechanically alloyed aluminum (MA-Al) [17–19]. However, little is known about the creep properties of metals with a high volume fraction (above 10 vol.%) of submicron unshearable dispersoids, such as dispersion-strengthened-cast aluminum (DSC-Al) containing 25 vol.% alumina dispersoids [20].

In the present study, the creep rate of DSC-Al is determined in both tension and compression as a function of temperature, stress and grain size. The experimental data are discussed in terms of three possible deformation mechanisms: diffusional creep, dislocation creep and cavitation. The measured creep rates for dislocation creep are then compared to the existing threshold stress models described above and to a new model developed in a theoretical companion article [1] for high dispersoid volume fractions, where the effect of dislocation pile-ups on the detachment threshold stress is considered.

2. EXPERIMENTAL PROCEDURE

Cast billets of DSC-Al consisting of 99.9% pure aluminum with 25 vol.% α-Al_2O_3 dispersoids (99.8% purity, mean diameter of $0.28 \pm 0.03 \ \mu m$) were supplied by Chesapeake Composite Corp. (New Castle, DE). Some of the billets were further extruded at 550°C with an extrusion ratio of 12. Smooth-bar tensile creep specimens (4.06 mm gage diameter and 25.40 mm gage length) and compressive cylindrical specimens (6.35 mm diameter and 12.70 mm length) were machined with their axis in the main billet or extrusion direction.

Tensile creep experiments were performed in air under constant-load conditions on specimens outfitted with an extensometer connected to a linear voltage displacement transducer (resolution $\pm 2.5 \ \mu m$). For compressive experiments, a superalloy compression-cage was used with boron-nitride-lubricated alumina platens. The platens displacement was transmitted by an extensometer to a linear voltage displacement transducer (resolution $\pm 1.0 \ \mu m$). The temperature was monitored with two thermocouples on the gage length and was maintained within a 2°C window. While only one specimen was used for each tensile stress level, a single specimen was used for up to four (increasing) compressive stress levels. The minimum creep rate associated with the first stress level was obtained after approximately 2% strain by linear regression on the last 0.5% strain data. The minimum creep rate for each subsequent stress level was obtained by linear regression on approximately 0.5% strain.

Cavitation tensile experiments were machined with larger gage diameter (4.70 mm) and length (63.50 mm) and smaller head volume than the nominal tensile samples, so that the ratio of the gage volume to the total sample volume was increased from 0.11 to 0.45. The sample density as a function of creep strain was determined by water displacement with Archimedes method. The relative error of the measurement on the modified tensile samples was estimated as 0.05% by measuring the same undeformed sample several times over a period of a few days. The relative error was slightly higher for the smaller compression samples. The change in density in the compression creep samples was assumed to be uniform throughout the sample, while the change in

the average density of the tensile sample was assumed to result solely from a change in gage density.

X-ray measurements were performed on a polished extruded specimen with a Rigaku RU200 diffractometer using CuKα radiation at an operating voltage and current of 50 kV and 150 mA, respectively. The sample was scanned through $2\theta = 35$–100 degrees at a rate of 10 deg/min with a sampling interval of 0.02 degree.

Samples were prepared for transmission electron microscopy (TEM) by a combination of mechanical grinding, dimpling and ion milling. Bulk material was first sectioned with a low-speed diamond saw and ground to a thickness of approximately 400 μm. Disks with a 3 mm diameter were then punched and dimpled with a 3 μm diamond slurry to a thickness of less than 50 μm. Finally, thinning to perforation was conducted using a Gatan Dual Ion Mill operating at 6 kV on a cooled sample stage. The electron-transparent samples were observed in a JEOL 200 CX transmission electron microscope operating at 200 kV.

3. EXPERIMENTAL RESULTS

As reported in an earlier paper [20], the as-cast DSC-Al specimens exhibit unsintered alumina dispersoids fully infiltrated by aluminum, and the matrix grain size is very large, in the range of millimeters to centimeters, because the ingots were directionally solidified. Extrusion results in an improved dispersoid distribution and a drastic refinement of the grains, which have an average length of 1.3 μm and an aspect ratio of about unity [20]. X-ray diffraction also showed that the extruded material exhibits a strong $\langle 111 \rangle$ texture, as also reported in other extruded dispersion-strengthened aluminum materials [19]. As expected from Zener pinning, the alumina dispersoids were located with higher frequency at grain boundaries than within the grains. The material is extremely resistant to grain growth and recrystallization: annealing for about 6 days at 650°C, corresponding to a homologous temperature of 0.99, leads to a grain size (about 1.8 μm) almost the same as in the as-extruded condition.

The minimum creep rate in tension is plotted as a function of stress for large-grained DSC-Al in Fig. 1(a) and for fine-grained DSC-Al in Fig. 1(b). Using the power-law equation [equation (1)] to describe the stress dependence of the minimum creep rate, the apparent stress exponents range from $n' = 9$ to $n' = 12$ for the large-grained material and from $n' = 10$ to $n' = 16$ for the fine-grained material (Table 1). These values are much higher than the bulk stress exponent for power-law creep of pure, unreinforced aluminum ($n = 4.4$ [21]). Also, the minimum creep rate for the large-grained material at a given stress is higher than the minimum creep rate for the fine-grained material at the same stress, and

this difference decreases as the temperature increases (Fig. 1). For the large-grained material, the apparent activation energy determined from equation (1) ranges from $Q' = 263$ kJ/mol for a tensile stress $\sigma = 42$ MPa to $Q' = 151$ kJ/mol for $\sigma = 100$ MPa. The apparent activation energy for the fine-grained
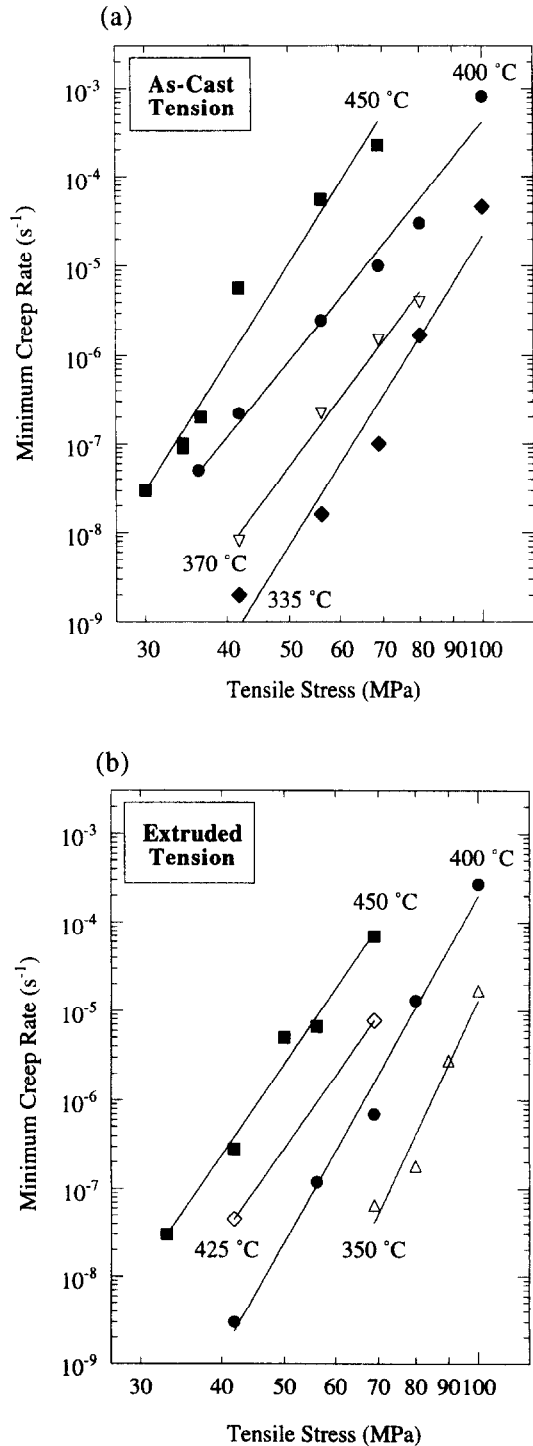

Fig. 1. Minimum creep rate as a function of tensile stress at different temperatures for (a) large-grained DSC-Al and (b) fine-grained DSC-Al.

Table 1. Tensile and compressive apparent stress exponents n' determined from equation (1) for as-cast, large-grained and extruded, fine-grained DSC-Al

Temperature (°C)	Tension		Compression	
	As-cast	Extruded	As-cast	Extruded
335	12			
350		16		
370	10			
400	9	13	22	23†, 9‡
425		10		
450	11	11	28	22†, 9‡
500				10

†High-stress value, ‡low-stress value.

material ranges from $Q' = 402$ kJ/mol for $\sigma = 42$ MPa to $Q' = 193$ kJ/mol for $\sigma = 100$ MPa.

The minimum creep rate in compression is plotted as a function of stress in Fig. 2(a, b) for both the as-cast, large-grained materials and the extruded, fine-grained materials. As summarized in Table 1, the apparent stress exponents at 400°C and 450°C for large-grained DSC-Al [$n' = 22$ and $n' = 28$, respectively, Fig. 2(a)] are similar to those for the fine-grained material at stresses above about $\sigma = 70$ MPa [$n' = 23$ and $n' = 22$, respectively, Fig. 2(b)]. However, for fine-grained DSC-Al at stresses below about $\sigma = 70$ MPa, the apparent stress exponent is much lower [$n' = 9$, Fig. 2(b)]. The minimum creep rate for large-grained DSC-Al is higher than for fine-grained DSC-Al for all stresses at 400°C; however, at 450°C, it is lower for fine-grained DSC-Al in the low stress regime. Finally, the apparent activation energies Q' calculated using the limited data in Fig. 2 (two to three data points) are on the order of 400–500 kJ/mol for both large- and fine-grained materials for stresses of $\sigma = 56$–85 MPa.

Figure 3 shows the relative change in density as a function of creep strain for samples tested at 400°C at a stress of 82 MPa. Except at low strains, density is constant, within experimental error, for both large- and fine-grained samples tested in compression. On the other hand, the density of the samples tested in tension decreased significantly with increasing strain. Figure 4(a)–(c) shows TEM micrographs of fine-grained DSC-Al crept at 450°C under a tensile stress of 33 MPa. These micrographs give examples of a typical feature observed in these and other samples, i.e. a dislocation pile-up interacting with a dispersoid.

4. DISCUSSION

4.1. Deformation mechanisms

As shown in Figs 1 and 2, both the loading direction and the thermo-mechanical treatment have a strong effect on the minimum creep rate of DSC-Al: creep is faster in tension than in compression for both materials at all stresses; and the extruded material creeps more slowly than the as-cast material, except at low stresses. Extrusion has two main effects on the matrix: it refines the grains from millimeter size to micron size and it introduces a strong $\langle 111 \rangle$ texture.

Texture influences the Taylor factor M, which has a value $M = 3.06$ [22] for f.c.c. materials with randomly oriented grains such as as-cast DSC-Al, and $M = 3.6$ [19] for fine-grained aluminum materials with a strong $\langle 111 \rangle$ fiber texture in the extrusion direction, such as extruded DSC-Al. Considering only the data at 400°C and 450°C for which both large- and fine-grained samples were tested in tension as well as in compression, we plot in Fig. 5 (a), (b) the minimum shear creep rate ($\dot{\gamma} = \sqrt{3} \cdot \dot{\epsilon}$) as a function of the resolved shear stress ($\tau = \sigma/M$). In these plots, most of the data merge for both as-cast and extruded materials, indicating that the improved creep resistance of the extruded materials observed in Figs 1 and 2 is due to texture; however, at low stresses the extruded, fine-grained material is weaker than the as-cast material and displays a lower stress exponent.

To correlate these experimental observations with theoretical models for creep deformation, it is necessary to first identify the mechanisms that contribute to the deformation. Time-dependent flow of material can occur by dislocation motion (power-law creep), by vacancy flow and grain boundary sliding (diffusional creep), or by pore nucleation and growth (cavitation). Depending on the grain size and testing mode, more than one of these three mechanisms may be operative and the total creep rate in the sum of the contributions from these independent mechanisms. The possible deformation mechanisms for large-grained and fine-grained DSC-Al under different loading conditions are listed in Table 2. The number of mechanisms is reduced from three (for the fine-grained materials in tension) to one (for the large-grained material in compression) by considering two features. First, because the grain size of the large-grained material is in the millimeter range, diffusional creep is not expected for either loading condition [21]. Second, irrespective of grain size, cavitation is not expected for compressive loading, as confirmed by experimental data shown in Fig. 3. From Table 2 and the creep data in Fig. 5(a), (b), it is possible to correlate experimental observations with a specific mechanism, as described in the following.

First, we examine the deformation mechanisms in compression, where the only possible mechanism for the large-grained material is dislocation creep. Since

that mechanism is not a function of grain size, it is possible to compare the large-grained and the fine-grained material in compression and assess the contribution of diffusional creep to the total deformation in the fine-grained material. At high stress levels, the stress exponents and creep rates are
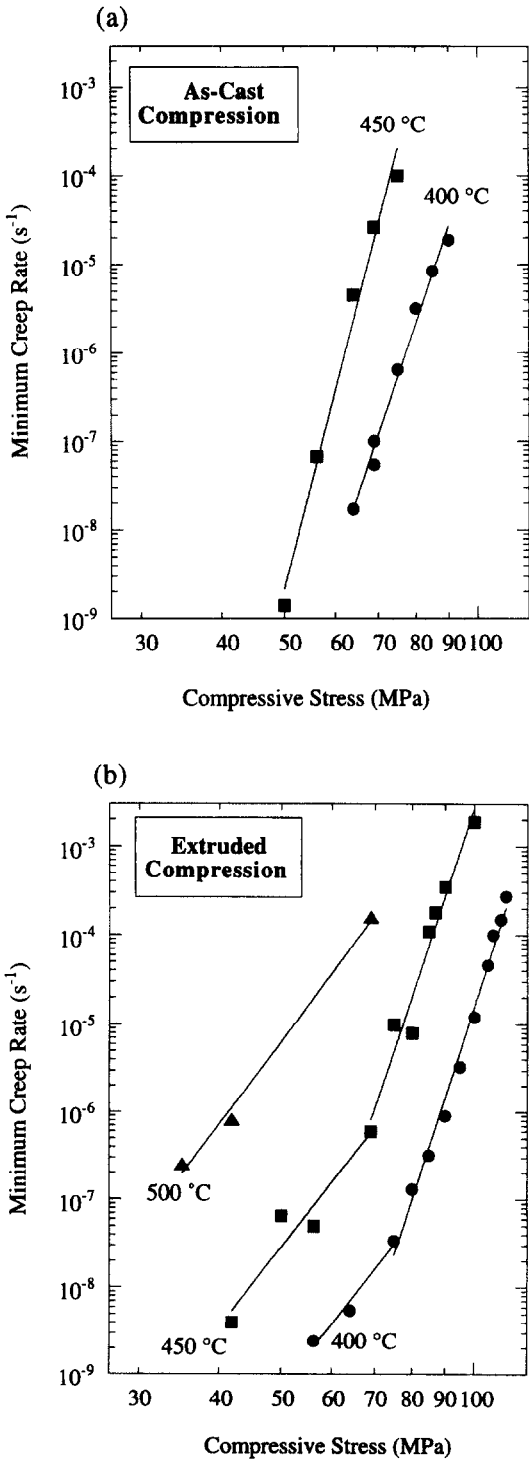
(a)

(b)

Fig. 2. Minimum creep rate as a function of compressive stress at different temperatures for (a) large-grained DSC-Al and (b) fine-grained DSC-Al.
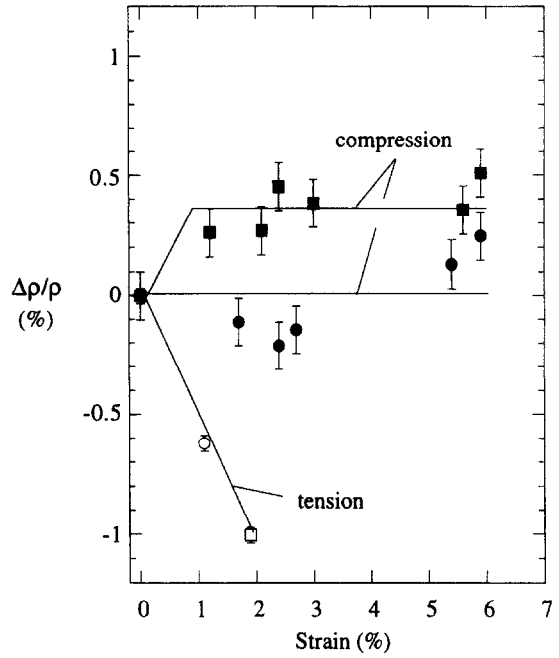

Fig. 3. Density as a function of creep strain for fine-grained (circles) and large-grained (squares) DSC-Al tested at 400°C at a stress of 82 MPa.

similar for both materials (Fig. 5 and Table 1); thus, the fine-grained material deforms by dislocation creep as well. However, at low stresses, the lower stress exponent and higher strain rate for the fine-grained material indicate that diffusional creep is the dominant deformation mechanism, albeit with a significant threshold stress since the apparent stress exponent ($n' = 9$–10) is much higher than the bulk value ($n = 1$–2).

Next, we consider the deformation mechanisms active in tension. Whereas only dislocation creep is possible in compression for the large-grained material, cavitation also occurs in tension (Fig. 3). For the large-grained material, the stress exponent is lower and the strain rate is higher in tension than in compression [Table 1, Fig. 5(a), (b)], as expected if a different mechanism (i.e. cavitation) is dominant in tension. The fine-grained material in tension exhibits a similar behavior as in compression [Fig. 5(a), (b)], indicating that cavitation is also the dominant mechanism for the fine-grained material in tension. In summary, the dominant deformation mechanisms deduced above are highlighted in bold characters in Table 2.

4.2. Threshold stress

We focus our discussion on the threshold stress for dislocation creep, for which existing models are summarized in the Introduction and a new model is presented in the theoretical companion article [1] for materials with high dispersoid volume fractions such as DSC-Al. As described in the preceding section, dislocation creep is the dominant mechanism for all

(a)

(b)

(c)

Fig. 4. (a)–(c) TEM micrographs of extruded, fine-grained DSC-Al crept at 450°C under a stress of 33 MPa and cooled under load showing pile-ups of dislocations (arrows) interacting with alumina dispersoids (A).
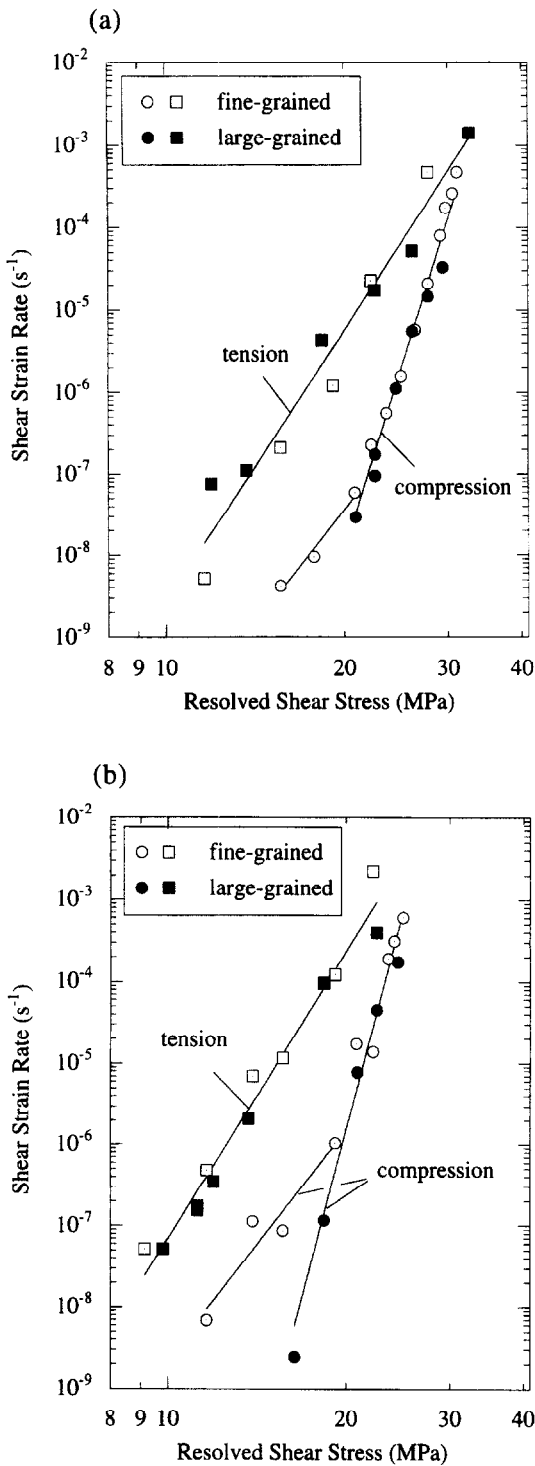
(a)

(b)

Fig. 5. Minimum shear creep rate ($\dot{\gamma} = \sqrt{3} \cdot \dot{\epsilon}$) as a function of the resolved shear stress ($\tau = \sigma/M$) for large-grained and fine-grained DSC-Al tested in tension and compression, (a) at 400°C and (b) at 450°C.

compressive stresses in the large-grained material and for high compressive stresses in the fine-grained material. The threshold stress for dislocation creep can be determined from the experimental data by plotting $\dot{\epsilon}^{1/n}$ as a function of σ, according to equation

(1). As shown in Table 3, the choice of the bulk stress exponent n can significantly affect the calculated value of the threshold stress. A possible approach is to choose the bulk stress exponent which produces the best linear fit to the data. Another approach is to select n based on the active deformation mechanism and the microstructure. For dislocation creep, three values of n are possible: $n = 3$ for creep controlled by viscous glide [23], $n = 5$ for creep by dislocation climb [24–26], and $n = 8$ for creep under constant structure [27, 28]. The experimentally determined stress exponent for pure aluminum, $n = 4.4$ [21], is intermediate between the values for dislocation glide and climb.

The value $n = 4.4$ is an appropriate choice for the as-cast, large-grained material which is expected to deform with a varying substructure; as shown in Table 3, the threshold stress values determined with $n = 3–5$ are quite similar. For the fine-grained materials, data fitted with $n = 4.4$ or $n = 8$ deviate from linearity at low stresses because of the effect of diffusional creep [29]. For stress levels above $\sigma = 65$ MPa, both stress exponents yield linear fits of similar quality, so that the appropriate stress exponent cannot be distinguished solely from the data. As pointed out by Lin and Sherby [28] for recrystallized dispersion-strengthened metals deforming by dislocation creep, dispersoids not only impart a threshold stress, they also refine the grain structure by Zener pinning, thereby increasing the creep strength and stress exponent (constant structure $n = 8$) by preventing the formation of subgrains (variable structure $n = 3–5$). For the fine-grained material, the grain size $d_g = 1.3$ μm is, except at the highest stresses at 400°C, smaller than the equilibrium subgrain size λ_{sg} given by Ref. [30] as

$$\frac{\lambda_{sg}}{b} = 23 \frac{\sigma}{G} \tag{7}$$

where b is the matrix Burger's vector and G is the matrix shear modulus. Thus, the fine-grained material is expected to deform with a constant structure, given by the grain size, with a bulk stress exponent $n = 8$. The experimentally determined threshold stress corresponding to the most likely controlling deformation mechanism (taking into account the microstructure) is underlined in Table 3. While the use of $n = 4.4$ for both grain sizes leads to similar threshold values for σ_{th}/M (Fig. 5), the compressive threshold stresses σ_{th} are similar for large- and fine-grained materials if constant

Table 2. Possible active deformation mechanisms (dominant mechanisms are highlighted in bold)

	Tension	Compression
Fine-grained	Dislocation	**Dislocation**[†]
	Diffusion	**Diffusion**[‡]
	Cavitation	
Large-grained	Dislocation	**Dislocation**
	Cavitation	

†At high stresses, ‡at low stresses.

Table 3. Experimentally determined compressive threshold stress (in MPa) for different stress exponents n

	Large-grained materials				Fine-grained materials*			
T (°C)	$n = 3$	$n = 4.4$	$n = 5$	$n = 8$	T (°C)	$n = 3$	$n = 4.4$	$n = 5$	$n = 8$
400	64	$\underline{59}$	57	47	400	79	74	72	$\underline{61}$
450	52	$\underline{50}$	48	42	450	70	65	63	$\underline{52}$

*Determined for stresses above 70 MPa.

substructure, i.e. $n = 8$, is assumed for the fine-grained material.

These experimental threshold values can now be compared to theoretical model predictions for the threshold stress [equations (3)-(6)], which are all expressed as a fraction of the Orowan stress (equation (3) in Ref. [1]), calculated using materials constants from Ref. [21] and $M = 3.06$ [22] for the large-grained material with randomly oriented grains or $M = 3.6$ [19] for the textured, fine-grained material. For the general climb model [equation (4)], a ratio $\kappa = 1/2$ determined by Ref. [10] for 25 vol.% of cubical dispersoids is used. For cooperative climb [equation (5)], the applied stress is assumed to be $0.67 \cdot \sigma_{or}$. First, since all climb mechanisms act in parallel, the overall climb threshold stress σ_{climb} is the smallest of the three climb thresholds [equations (3)-(5)], i.e. general climb at both 400°C and 450°C. Second, since the climb and detachment processes act in series, the predicted threshold stress (underlined in Table 4) is the greater of σ_{climb} and σ_{det}. At both 400°C and 450°C, the predicted threshold stress is then the detachment stress, which is calculated from equation (6) with a relaxation factor $k = 0.80$ determined by Rösler et al. [19] for the Al-Al$_2$O$_3$ system. Comparing this predicted value with the experimentally determined threshold stress values, Table 4 shows that the experimental values are higher by 45–90% than those calculated for the detachment stress [equation (6)]; the discrepancy would be even larger if $n = 4.4$ was used to determine the threshold stress of the fine-grained materials (Table 3).

The difference between experimental and theoretical threshold values (24–28 MPa at 400°C and 16–20 MPa at 450°C) is too large to be explained by errors in the materials constants and geometric parameters used in the threshold equations [equations (3)-(6)] and the Orowan stress. Rather, we believe that the very high threshold stress values in DSC-Al are due to the interaction between the detaching dislocation and dislocations piled up at dispersoids. As shown in the theoretical companion

article [1], pile-ups exert a stress σ_p on the detaching dislocation which can be superimposed to the detachment threshold stress σ_{det} [equation (6)], leading to a net threshold stress σ_{th}:

$$\sigma_{th} = \sigma_{det} + \sigma_p. \qquad (8)$$

TEM observations confirm the existence at dispersoids of dislocation pile-ups in DSC-Al [Fig. 4 (a)–(c)], which are calculated to contain an average number of dislocations $N = 5$ at the threshold stress [equation (10) in Ref. [1]].

Table 5 lists for coarse-grained DSC-Al the pile-up stresses (calculated from equation (23) in Ref. [1]) as a function of the number N of dislocations in the pile-ups and of the number P of dispersoids being cooperatively bypassed by the dislocations. For values of $N = 5$, calculated above for DSC-Al, and for $P = 5$, the correct sign and magnitude are predicted for the pile-up stress at both temperatures, i.e. $\sigma_p = 22$ MPa at 400°C and $\sigma_p = 20$ MPa at 450°C; similar result are found for fine-grained DSC-Al. We note that, while P is an adjustable parameter, the predictions for the pile-up stress do not vary significantly for $3 \leqslant P < \infty$ (Table 5); it seems reasonable to assume that, in DSC-Al with very high volume fractions of dispersoids, some cooperative climb ($P \geqslant 3$) is taking place. While the good quantitative agreement between experiment and theoretical predictions may be fortuitous because of the many simplifying assumptions in the model and the uncertainties associated with materials constants such as k and n, we believe that the model presented in our companion paper [1] is a reasonable explanation for the anomalously high threshold stresses observed in DSC-Al.

In summary, the experimental threshold stresses for DSC-Al are significantly higher than predicted with existing models considering a single dislocation interacting with one or more dispersoids. The model presented in Ref. [1] for materials with high volume fractions of dispersoids such as DSC-Al considers pile-ups of dislocations forming at dispersoids, as

Table 4. Compressive threshold stress values (in MPa) as predicted from existing models (underlined) and as experimentally determined (σ_{th}). A bulk stress exponent $n = 4.4$ is used for large-grained DSC-Al and $n = 8$ for fine-grained DSC-Al

Grain size	Temp.	σ_{or}	σ_{loc}	σ_{gen}	σ_{coop}	σ_{climb}	σ_{det}	σ_{th}	$\sigma_{th} - \sigma_{det}$
	(°C)	[Eq. (3)†]	[Eq. (3)]	[(Eq. (4)]	[(Eq. (5)]	(‡)	[Eq. (6)]	(§)	
Large	400	106	42	21	33	21	$\underline{31}$	59	28
Large	450	102	41	20	32	20	$\underline{30}$	50	20
Fine	400	125	50	25	39	25	$\underline{37}$	61	24
Fine	450	120	48	24	37	24	$\underline{36}$	52	16

†In Ref. [1]; ‡lowest of σ_{loc}, σ_{gen}, σ_{coop}; §experimental value.

Table 5. Tensile pile-up stress σ_p [equation (8)] as a function of the parameters N and P, as determined in the theoretical companion article [1]

	$N = 1$	$N = 2$	$N = 3$	$N = 4$	$N = 5$	$N = 6$
400°C, 64 MPa						
$P = 1$	0	−2.0	−7.9	−17.4	−28.6	−39.1
$P = 3$	0	9.6	14.5	15.1	13.8	13.3
$P = 5$	0	11.8	19.0	21.6	22.3	23.8
$P = \infty$	0	15.3	25.7	31.3	35.0	39.4
450°C, 50 MPa						
$P = 1$	0	0.3	−4.4	−12.3	−20.6	−25.8
$P = 3$	0	9.7	13.4	13.4	12.9	16.0
$P = 5$	0	11.6	17.0	18.5	19.6	24.4
$P = \infty$	0	14.4	22.3	26.2	29.6	36.9

observed experimentally by TEM [Fig. 4 (a)–(c)]. The model then makes predictions for the threshold stress which are in good agreement with the experimental values.

4.3. Activation energy

As for the above discussion of the threshold stress, we consider the activation energy for dislocation creep only, i.e. for compressive data at all stresses for the large-grained material and at high stresses for the fine-grained material. The apparent activation energy Q' for a material exhibiting a threshold stress given by one of the existing models reviewed in the Introduction [equations (3)–(6)], is given in Ref. [1] as

$$Q' = Q - RT\left[1 + \frac{T}{G}\frac{dG}{dT}\left(n\frac{\sigma}{\sigma - \sigma_{th}} - 1\right)\right]. \quad (9)$$

Equation (9) is valid if the only temperature-dependent term in the threshold stress [equations (3)–(6)] is the shear modulus G. Using materials data and the activation energy for pure aluminum $Q = 142$ kJ/mol given in Ref. [21] as well as a representative value $\sigma_{th}/\sigma = 0.75$, equation (9) predicts an activation energy $Q' = 178$ kJ/mol, much lower than the observed value for DSC-Al ($Q' = 400$–500 kJ/mol).

In the model presented in the theoretical companion article [1] for materials with high volume fractions of dispersoids, the threshold stress is a function of two temperature-dependent variables: the shear modulus from the Orowan stress and the pile-up stress σ_p [equation (8)]. With increasing temperature, the number of dislocations in the pile-ups (and thus the magnitude of σ_p) are expected to decrease, because dislocations can escape from the pile-ups by climb more readily at elevated temperature. Defining the ratio of the pile-up stress σ_p to the Orowan stress σ_{or} as the dimensionless parameter C_2, the apparent activation energy was then derived in Ref. [1] as

$$Q'' = Q' - nRT^2\frac{\sigma_{or}}{\sigma - \sigma_{th}}\frac{dC_2}{dT} \quad (10)$$

where dC_2/dT is negative. While modeling the escape by climb of dislocations from stressed pile-ups could in principle yield a value for dC_2/dT, we do not attempt this task owing to the large number of unverifiable assumptions necessary. Rather, using a representative value $\sigma_{or}/\sigma = 1.5$, we fit equation (10)

to the experimental data ($Q' = 400$–500 kJ/mol) to find a value $dC_2/dT = 0.022$–0.032 K^{-1}. The inverse value $(dC_2/dT)^{-1} = 312$–454 K represents the temperature span over which the pile-up stress decreases by an increment equal to the Orowan stress, i.e. from a maximum value $\sigma_p = \sigma_{or}$ ($C_2 = 1$) to a minimum value $\sigma_p = 0$ ($C_2 = 0$). The value of this temperature span is physically plausible, since it is comparable to the temperature interval bounded by the temperatures $T = 0.6 \cdot T_m$ (where dislocation climb starts to occur at rates comparable to the deformation rate and C_2 is close to unity) and $T = T_m$ (where dislocation climb is very rapid and C_2 is close to zero), where $T_m = 933$ K is the melting point of aluminum.

In summary, as for the threshold stress, the experimental apparent activation energies for DSC-Al deforming by dislocation creep are much higher than predicted by models considering a single dislocation interacting with dispersoids. In the model presented in the theoretical companion article [1] for materials with high dispersoid contents where pile-ups contribute to the threshold stress, this contribution decreases with increasing temperature, as dislocations escape the pile-ups by climb. A corrected activation energy is then predicted, which can be fitted to experimental data for DSC-Al so that the only adjustable parameter dC_2/dT falls within physically plausible values.

5. SUMMARY

• The tensile and compressive creep properties of DSC-Al containing 25 vol.% of 0.28 μm Al$_2$O$_3$ dispersoids were studied between 335°C and 500°C for large- and fine-grained materials. The creep strength and creep stress- and temperature-sensitivity are significantly higher than those of pure aluminum, indicating that the dispersoids impede dislocation creep and diffusional creep.

• Density measurements show that, for both large- and fine-grained materials, cavitation occurs in tension but not in compression. Since the tensile creep strength and the apparent stress exponent are significantly lower in tension than in compression, cavitation is the dominant deformation mechanism in the minimum secondary creep regime in tension.

• In compression, the dominant deformation mechanism for the fine-grained materials at low

stresses is diffusional creep. However, both the high apparent stress exponent of about $n' = 9$ and the low strain rates indicate that diffusional creep is strongly inhibited by the dispersoids.

● In compression, the dominant deformation mechanism is dislocation creep at all stresses for the large-grained material and at high stresses for the fine-grained material. Apparent stress exponents larger than $n' = 20$ are measured at 400°C and 450°C, corresponding to threshold stress values of $\sigma_{th} = 50$–61 MPa. These threshold values are significantly higher than predictions from existing climb or detachment dislocation models.

● When the dispersoid content is above about 10 vol.%, dislocation pile-ups are expected to form at dispersoids (as observed by TEM) and so directly exert a net to stress upon the dislocations pinned at the dispersoids, which control the threshold behavior. A new model for high volume fraction dispersion-strengthening, presented in the theoretical companion article [1], calculates this pile-up stress acting upon the detaching dislocations and predicts a range of threshold stresses in good agreement with our experimental data for DSC-Al deforming by dislocation creep.

● The same model predicts that the number of dislocations in the pile-ups, and thus the pile-up stress contribution to the threshold stress, decrease with increasing temperature. The resulting apparent activation energy is then much higher than for materials with low dispersoid contents where no pile-up exist. Experimental activation energies for DSC-Al are fitted to these predictions with a single adjustable parameter, which takes a physically plausible value.

REFERENCES

1. Dunand, D. C. and Jansen, A. M., *Acta mater.*, 1997, **45**, 4583
2. Gibeling, J. C. and Nix, W. D., *Mater. Sci., Engng*, 1980, **45**, 123.
3. Arzt, E., *Res. Mech.*, 1991, **31**, 399.
4. Arzt, E., *Mechanical Properties of Metallic Composites*, ed. S. Ochiai. Marcel Dekker, Inc., New York, 1994, p. 205.
5. Raj, S. V., *Mechanical Properties of Metallic Compositese*, ed. S. Ochiai. Marcel Dekker, Inc., New York, 1994, p. 97.
6. Brown, L. M. and Ham, R. K., *Strengthening Methods in Crystals*, ed. A. Kelly and R. B. Nicholson. Elsevier, Amsterdam, 1971, p. 9.
7. Shewfelt, R. S. W. and Brown, L. M., *Phil. Mag.*, 1974, **30**, 1135.
8. Shewfelt, R. S. W. and Brown, L. M., *Phil. Mag.*, 1977, **35**, 945.
9. Lagneborg, R., *Scripta metall.*, 1973, **7**, 605.
10. McLean, M., *Acta metall.*, 1985, **33**, 545.
11. Srolovitz, D. J., Luton, M. J., Petkovic-Luton, R., Barnett, D. M. and Nix, W. D., *Acta metall.*, 1984, **32**, 1079.
12. Arzt, E. and Wilkinson, D. S., *Acta metall.*, 1986, **43**, 1893.
13. Rösler, J. and Artz, E., *Acta metall. mater.*, 1990, **38**, 671.
14. Ansell, G. S., *Trans. AIME*, 1959, **215**, 294.
15. Milicka, K., Cadek, J. and Rys, P., *Acta metall.*, 1970, **18**, 733.
16. Clauer, A. H. and Hansen, N., *Acta metall.*, 1984, **32**, 269.
17. Oliver, W. C. and Nix, W. D., *Acta metall.*, 1982, **30**, 1335.
18. Kucharova, K. and Orlova, A., *Mater. Sci. Engng*, 1988, **A102**, 201.
19. Rösler, J., Joos, R. and Artz, E., *Metall. Trans.*, 1992, **23A**, 1521.
20. Redsten, A. M., Klier, E. M., Brown, A. M. and Dunand, D. C., *Mater. Sci. Engng*, 1995, **A201**, 88.
21. Frost, H. J. and Ashby, M. F., *Deformation-Mechanism Maps: The Plasticity and Creep of Metals and Ceramics*. Pergamon Press, Oxford, 1982, p. 21.
22. Meyers, M. A. and Chawla, K. K., *Mechanical Metallurgy: Principles and Applications*. Prentice-Hall, Englewood Cliffs, NJ, 1984, p. 343.
23. Weertman, J., *J. appl. Phys.*, 1957, **28**, 1185.
24. Barrett, C. R. and Sherby, O. D., *Trans. ASM*, 1965, **233**, 1116.
25. Mohamed, F. A. and Langdon, T. G., *Acta metall.*, 1974, **22**, 779.
26. Weertman, J., *Creep and Fracture of Engineering Materials and Structures*, ed. B. Wilshire and D. R. J. Owen. Pineridge Press, 1984, p. 1.
27. Sherby, O. D., Klundt, R. H. and Miller, A. K., *Metall. Trans.*, 1977, **8A**, 843.
28. Lin, J. and Sherby, O. D., *Res. Mech.*, 1981, **2**, 251.
29. Pichler, A. and Artz, E., *Acta Mater.*, 1996, **44**, 2751.
30. Raj, S. V. and Pharr, G. M., *Mater. Sci. Engng*, 1986, **81**, 217.